Environ Geol (2007) 53:849–859
DOI 10.1007/s00254-007-0698-6

ORIGINAL ARTICLE

Geoelectric resistivity sounding of riverside alluvial aquifer in an agricultural area at Buyeo, Geum River watershed, Korea: an application to groundwater contamination study

Yong-Hee Park · Seong-Jae Doh · Seong-Taek Yun

Received: 4 October 2006 / Accepted: 20 February 2007 / Published online: 13 March 2007

Abstract Twenty profiles of vertical electric soundings (VES) were obtained in a riverside alluvium at the Buyeo area, South Korea, to examine the variations of subsurface geology and associated groundwater chemistry. The combination of the VES data with the borehole data provided useful information on subsurface hydrogeologic conditions. The vestige of an ancient river channel (e.g. oxbow lake) was identified on the resistivity profiles by the lateral continuation of a near-surface perched aquifer parallel to the river. Such a perched aquifer is typically developed in the area with a clay-rich silty surface alluvium which prohibits the infiltration of oxygen. Therefore, groundwater below the oxbow lake shows a very low nitrate concentration and Eh values under the strong anoxic condition. The distribution of water resistivity is correlated with that of measured total dissolved solids concentration in groundwater, while the earth resistivity of the aquifer shows a significant spatial variation. It is interpreted that the earth resistivity of the aquifer is mainly controlled by the soil type rather than by the water chemistry in the study area.

Keywords Vertical Electric Sounding (VES) · Schlumberger array · Riverside alluvium · Aquifer geology · Water chemistry · Korea

S.-J. Doh (✉) · S.-T. Yun
Department of Earth and Environmental Sciences
and the Environmental Geosphere Research Laboratory (EGRL),
Korea University, Seoul 136-713, South Korea
e-mail: sjdoh@korea.ac.kr

Present Address:
Y.-H. Park
Department of Geophysics, Kangwon National University,
Chuncheon, Kangwon-Do 200-701, South Korea

Introduction

Groundwater of alluvial aquifers is one of the most important sources of water supply in rural agricultural areas. For an effective use and management of alluvial groundwater, it is very important to know the characteristics of aquifers (e.g. depth, spatial distribution, and geology) and the relationship between subsurface geology and groundwater quality. The water quality of alluvial aquifers in rural areas is highly sensitive to the use of agricultural chemicals (e.g. fertilizers, pesticides, and lime) and manure as well as to the geologic conditions (Burt et al. 1999; Kraft et al. 1999; Min et al. 2003; Chae et al. 2004). Two recent hydrochemical studies in Korea reported that groundwaters of riverside alluvial aquifers, including the present study area, were seriously contaminated by nitrate because of the excessive use of N-fertilizers and manure (Min et al. 2003; Chae et al. 2004).

Successful exploration, exploitation, and management of groundwater require a good knowledge of the spatial distribution of aquifer characteristics such as lithology, thickness, and hydraulic properties. Where such information is not available, geophysical surveys should be performed. Drilling and pumping tests are commonly used for evaluating aquifer characteristics; however, they are time- and cost-consuming (Yang and Lee 2002). Electrical resistivity is widely considered as a useful parameter for hydrogeological studies, because the value is mainly controlled by lithological conditions of the aquifer. It also can be useful in correlating lithological facies between wells (Fred 1993; El Gamili et al. 2001). Thus, the geoelectrical columns and cross-sections, deduced from the vertical electric sounding (VES), can provide an effective way to image the vertical and lateral variations of subsurface hydrolithology with a minimum need of observation wells.

However, resistivity values are also sensitive to the porosity and water content of the aquifer, as well as to the mineralization and salinity of groundwater (McNeill 1980; Parasnis 1997; Pozdnyakova et al. 2001; Choudhury and Saha 2004). Because of such complicated factors affecting the resistivity values, the lithology and water quality effects cannot be differentiated by the geoelectric resistivity survey alone (Choudhury and Saha 2004). For an effective use of geoelectric resistivity data to the hydrogeologic study, the correlation with hydrochemistry data is required. From this viewpoint, the riverside alluvium alongside the Geum River, Korea, was selected for this study because detailed hydrochemistry data have been reported by Chae et al. (2004).

The main purpose of the present study is to provide information on the subsurface lithology and groundwater occurrence for hydrogeologic interpretations using an integration of the geoelectric resistivity measurements, direct observation of lithology from boreholes information, and hydrochemical data obtained from irrigation wells. A discussion on the relationship between the earth resistivity, obtained on the land surface, and the water resistivity, measured directly from water samples is included to evaluate the usefulness and limitation of the earth resistivity data in subsurface hydrogeologic investigation.

Geologic and hydrologic settings

The study area is in a watershed of the Geum River, the third biggest river in South Korea (Fig. 1a). The study area has a temperate monsoon climate with an average annual precipitation of about 1,300 mm, of which more than 60% occurs during the summer months from June to September. Cultivation of various crops has been active for thousands of years. Recently, agricultural activities are year-round in the study area, owing to the use of greenhouses in winter season. A large amount of synthetic fertilizers and manure is applied, which severely pollutes alluvial groundwater (Chae et al. 2004). The Geum River in the study area meanders from north to south. The alluviums were formed by repetitive point-bar accretion and channel migration due to meandering of the river (Rhee et al. 2002). Comparison of a present-day topographic map with that printed in 1923 shows a considerable migration (westerly up to 400 m) of the river channel in the study area over the past 80 years (Chae et al. 2004).

The point-bar sediments overlie Jurassic granitic basement and have a thickness of ~25 m in the study area. Surface alluvium along the present river forms a narrow band composed mainly of medium to coarse sand without silt (Fig. 1b). On the other hand, silt-rich sediments (of various thicknesses) covered most of the study area except for the area adjacent to the river due to frequent flooding events (Fig. 1b). According to the GPR and seismic survey, alluvium sediments are nearly horizontal or dip slightly toward the main channel and decrease in thickness with distance from the present channel (Kim et al. 2003). Groundwaters are pumped out from the sand aquifer for agricultural purposes. Piezometric data indicate that groundwater in the study area generally flows toward the river from the inland (Chae et al. 2004; Fig. 2a).

Hydrochemical data of alluvial groundwater in the study area can be clustered into Groups I, II, and III according to the chemical characteristics (Chae et al. 2004). The areal distribution of the clustered groups is shown in Fig. 2b. Group II waters occur in the area with a thick silt cover overlying the sand aquifer, and are characterized by very high levels of dissolved Fe (Iron) and Mn (Manganese). Such hydrochemistry indicates the formation of a strong anoxic condition in the aquifer. Group II waters also show very low concentration of NO_3, which might be caused by denitrification. Groundwaters of Groups I and III occur in the area without a thick silt cover and are highly influenced by surface agricultural activities. In particular, Group I waters contain very high concentrations of NO_3, SO_4, Ca, Mg, and K, due to the strong influence by fertilization and liming. Chae et al. (2004) pointed out that water chemistry in the riverside sandy area is also highly sensitive to the precipitation infiltration.

Methods

For this study, a total of 20 VES profiles were obtained in September and October 2003, using the OYO McOHM resistivity meter (model 2115A) with the Schlumberger configuration (M-AB-N). For each VES profile, the distance between the potential electrodes (MN) was gradually increased in steps starting from 0.5 m to 5 m to obtain a measurable potential difference. The half current electrode separation (AB/2) was usually increased in steps starting from 1 m to 100 m.

The interpretation of the VES data was conducted using the W-Geosoft commercial program WinSev6, which produces the resistivity model fitting the acquired field data with the least RMS-error between the observed and calculated resistivities. The method of iteration was performed until the fitting errors between field data and theoretical model curve fell less than 10%. Because the electric resistivity of sediments depends on lithology, water content, clay content, and salinity (McNeill 1980; Choudhury and Saha 2004), it is important to correlate the VES results with the lithological and hydrological information obtained from adjacent boreholes (e.g. Edet and Okereke 2002). Two boreholes B-1 and B-2, close to the VES stations

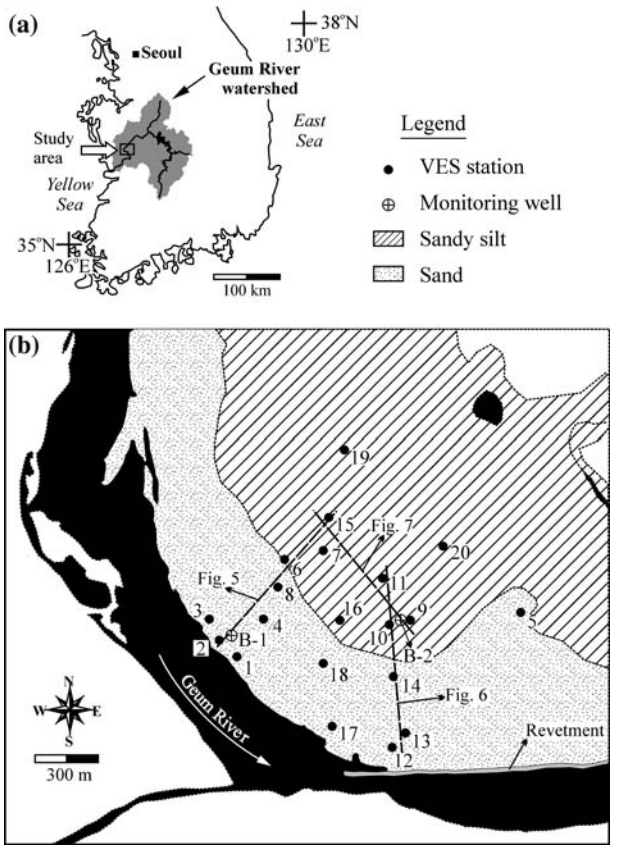

Fig. 1 **a** Location of the study area. **b** The sites of vertical electric sounding. Surface geology is also shown. *Dashed lines* denote the cross sections of interpreted-resistivity columns shown in Figs. 5, 6, and 7

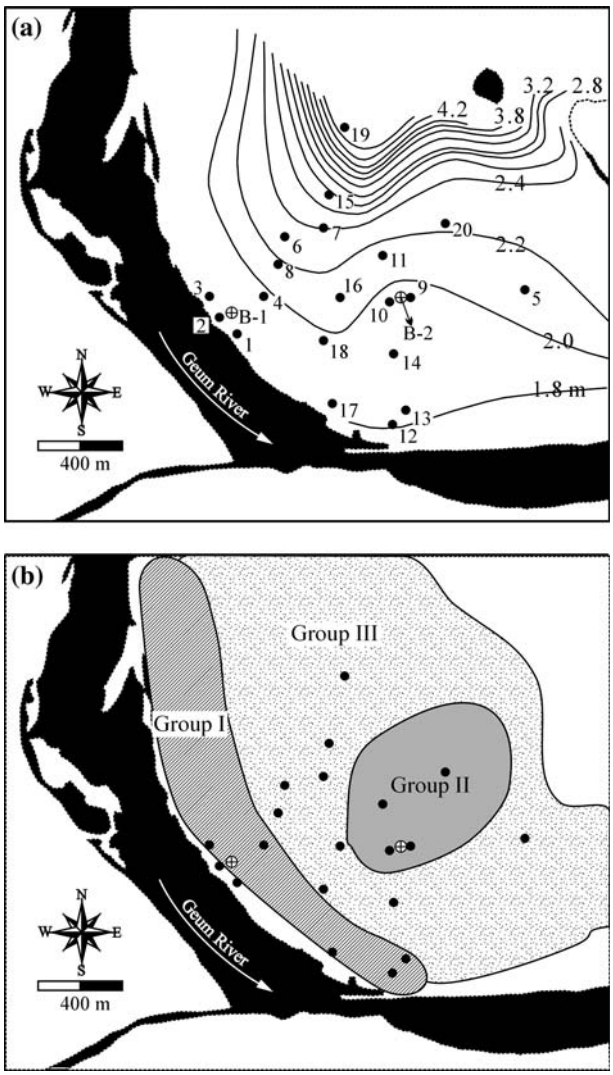

Fig. 2 **a** Equipotential lines (groundwater level contours) based on the piezometric data, and **b** an areal distribution of the clustered groups, based on the hydrochemistry data in 2002 (after Chae et al. 2004). *Black dots* indicate the VES locations

VES-2 and VES-9, respectively, were used for the correlation (Fig. 1b).

Results and discussions

VES profiles and borehole data

Figure 3 shows the VES curve for the site VES-2 that is at the southwestern part of the study area, adjacent to the Geum River. The results from VES-1 and VES-3 were very similar to that from VES-2, and thus are not shown here. The lithological variation, deduced from the borehole B-1, is shown on the right side of Fig. 3 for the correlation with the resistivity profile.

Based on the correlation between the three VES profiles (VES-1, VES-2, and VES-3) and the lithological information from the borehole (B-1), five major resistivity layers are recognized in the southwestern portion of the study area (Fig. 3). The topmost, relatively low resistivity (89 Ωm) layer is well correlated with the agricultural soil of sandy characteristics. The second resistivity layer shows the extremely wide range of resistivity values (90–1,807 Ωm) and can be interpreted as an unsaturated, sandy stratum intercalated with thin sub-layers of pebble or silt. The wide resistivity range within the second layer can be considered as the result of significant variability in the content of clay or water due to the variable grain size of strata. However, the lithologic data from the borehole (B-1) did not show a distinctive difference in grain size between the low resistivity (90 Ωm) zone and the high resistivity (1,434 and 1,807 Ωm) zone. Therefore, the upper low resistivity zone at depths from 2.7 to 4 m in Fig. 3 indicates the presence of a perched aquifer (or water-saturated zone) between unsaturated sandy strata at shallow depth. The third resistivity layer shows very low resistivities (below 45 Ωm) and is interpreted to coincide with a water-

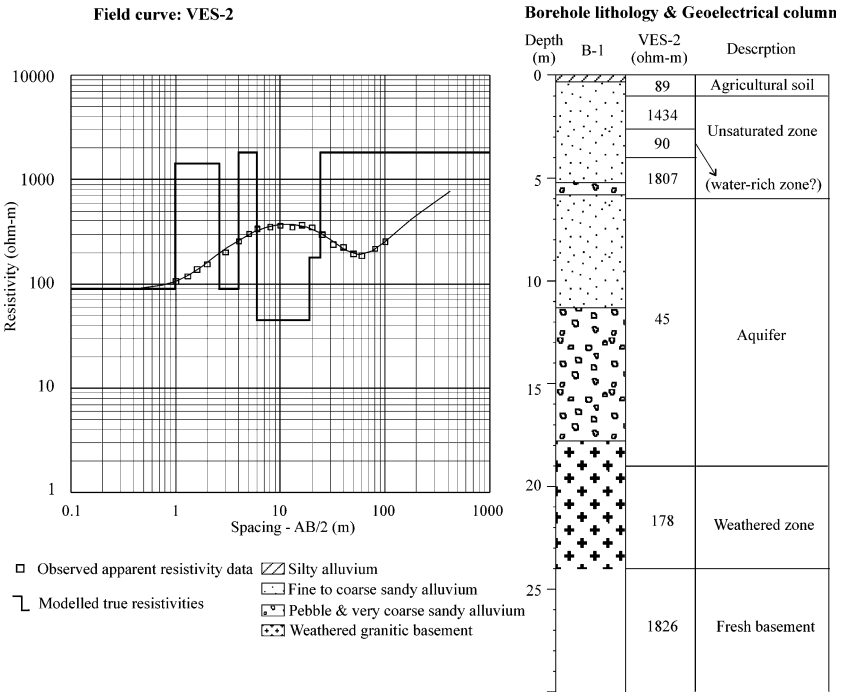

Fig. 3 Representative examples of the VES (*VES-2*) calibration with the lithology of the nearest borehole (*B-1*) in a sandy agricultural soil. *Squares* denote the observed apparent resistivity versus a half electrode separation (AB/2). The *solid curve*, superimposed on the *squares*, is the theoretical curve for the best fit model for the VES. The *thick line* is the interpretative modeled true resistivities

saturated sandy aquifer. The weathered granitic basement (the fourth layer) was identified at depths from 19 to 24 m by the more or less increased resistivity (178 Ωm). The fifth layer which has a high resistivity (up to 1,826 Ωm) is regarded as a fresh granitic basement.

Figure 4 shows the results obtained from the site of VES-9 near the borehole B-2, at the central part of the study area where a silty alluvium covers the surface. It is worth noting that the upper part of the B-2 is dominated by the silty alluvium (Fig. 4), while that of B-1 by a sandy alluvium (Fig. 3). The presence of a near-surface perched aquifer is also recognized by the very low resistivity (17 Ωm). This very low resistivity value is possibly due not only to the high water content (i.e. local saturated condition) but also a significant content of clay in a silty alluvium, as was also recognized by borehole logging (Fig. 4).

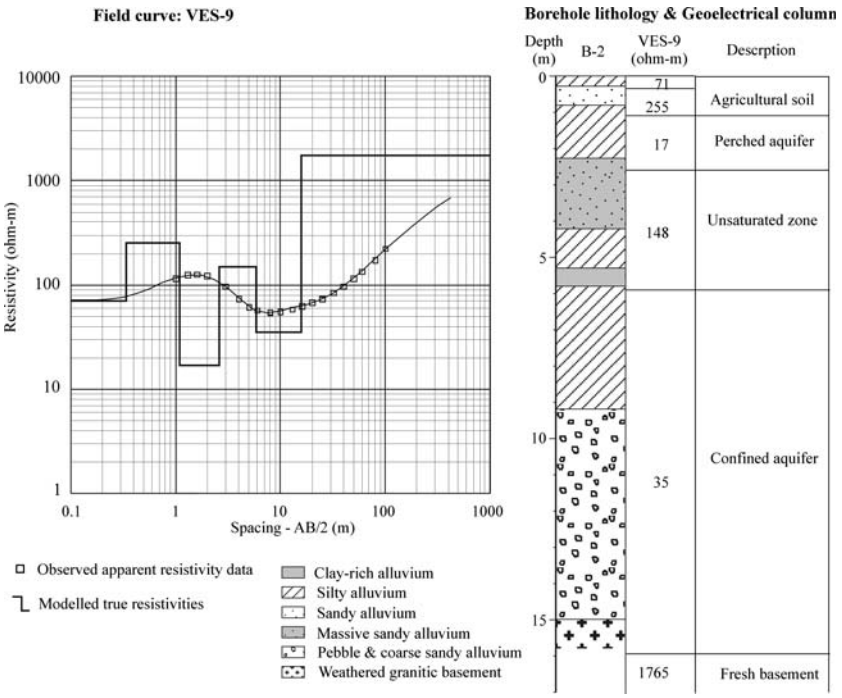

Fig. 4 Representative examples of the VES (*VES-9*) calibration with the lithology of the nearest borehole (*B-2*) in a silty agricultural soil. *Squares* denote the observed apparent resistivity versus a half electrode separation (*AB/2*). The *solid curve*, superimposed on the squares, is the theoretical curve for the best fit model for the VES. The *thick line* is the interpretative modeled true resistivities

The main groundwater table is identified at a depth of ~6 m by the low resistivity (35 Ωm). The high resistivity layer (up to 1,765 Ωm) occurs below ~16 m from the surface and coincides with a fresh granitic basement. A refraction and reflection seismic survey performed along a line (about 120 m long) in the center of the study area (Kim et al. 2003) showed that the depth of the groundwater table ranges from 6.5 to 10 m beneath the land surface and the fresh basement occurs at depth of about 25 m. Thus, the geoelectrical columns deduced from this VES survey show a good agreement with the results obtained from the previous seismic survey by Kim et al. (2003). In summary, inferred geoelectrical models for the study area are generally in good agreement with the results from lithologic logs and seismic survey.

Cross-sections deduced from VES data

Using the calibrated VES data, three geoelectrical cross-sections were constructed to reveal the lateral and vertical hydro-lithological variations in the study area (Figs. 5, 6, 7). Of them, two sections are oriented as NE–SW (Fig. 5) or N–S (Fig. 6), which are approximately transverse to the flow direction of the Geum River, while one section is oriented in a NW–SE direction which is approximately parallel to the river (Fig. 7).

The depth to the main groundwater table (i.e. thickness of the unsaturated zone) generally tends to progressively increase toward the river (Figs. 5, 6), which agrees well with the piezometric data shown in Fig. 2a. However, the main groundwater table at the VES-2 location nearest to the river was recognized at a significantly high level (~6 m deep) (Fig. 5). The river water level generally becomes higher during the post-monsoon period between September and October, during which the VES surveys were carried out for this study. Therefore, such increase of groundwater level at the VES-2 location possibly resulted from the direct inflow or pressure transmission of river water into adjacent agricultural land owing to the elevated level of the river. Such interpretations can be supported by the fact that the highly elevated groundwater table was never observed around the VES-12 location (Fig. 6), where the embankment and revetment were constructed along the riverside (Fig. 1b).

The resistivity value of unsaturated strata above the main groundwater table shows a distinctive contrast between the southwestern (or southern) part and the northeastern (or northern) part of the study area. The southwestern (or southern) part typically shows a thick layer of relatively high resistivities (450–2,004 Ωm), which are interpreted as medium to coarse sand layers (VES-2, VES-4, and VES-8 in Fig. 5; VES-12, VES-13, and VES-14 in Fig. 6). On the other hand, the northeastern (or northern) part shows the relatively low resistivity (113–430 Ωm) layers with a thin intercalation of high resistivity (687–850 Ωm) layer (VES-6, VES-7, and VES-15 in Fig. 5; VES-10, VES-9, and VES-11 in Fig. 6). These low resistivity layers can be interpreted as silt-dominant layers. The boundary between the high- and low-resistivity zones within unsaturated alluvium (i.e. boundary between northeastern (or northern) part and southwestern (or southern) part) matches well with that between sandy and silty agricultural soils on the surface (Fig. 1b). Therefore, the VES profiles in this study show that the boundary

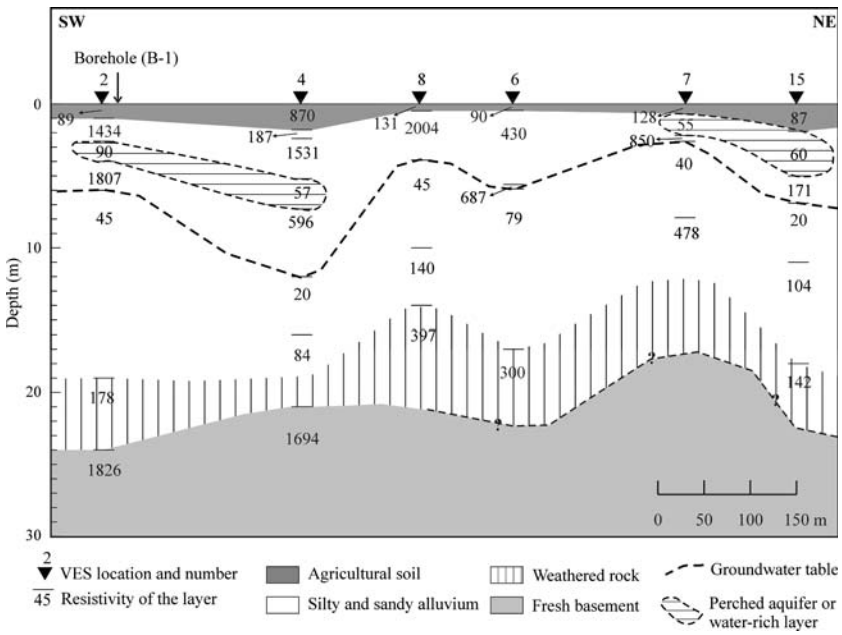

Fig. 5 A litho- and hydro-resistivity cross section with a NE–SW trend, transverse to the river. The location is shown in Fig. 1b. Vertical exaggeration is ×16

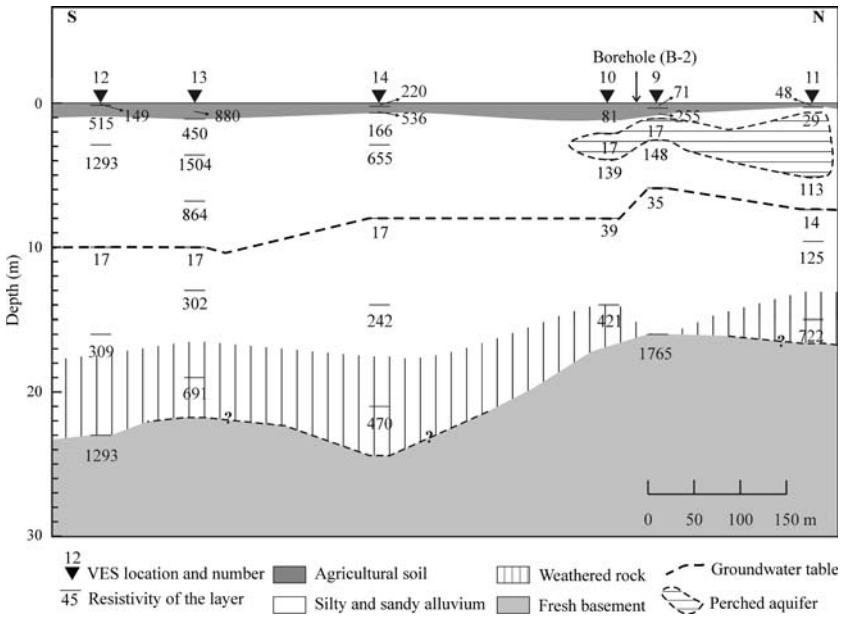

Fig. 6 A litho- and hydro-resistivity cross section with a N–S trend, transverse to the river. The location is shown in Fig. 1b. Vertical exaggeration is ×16

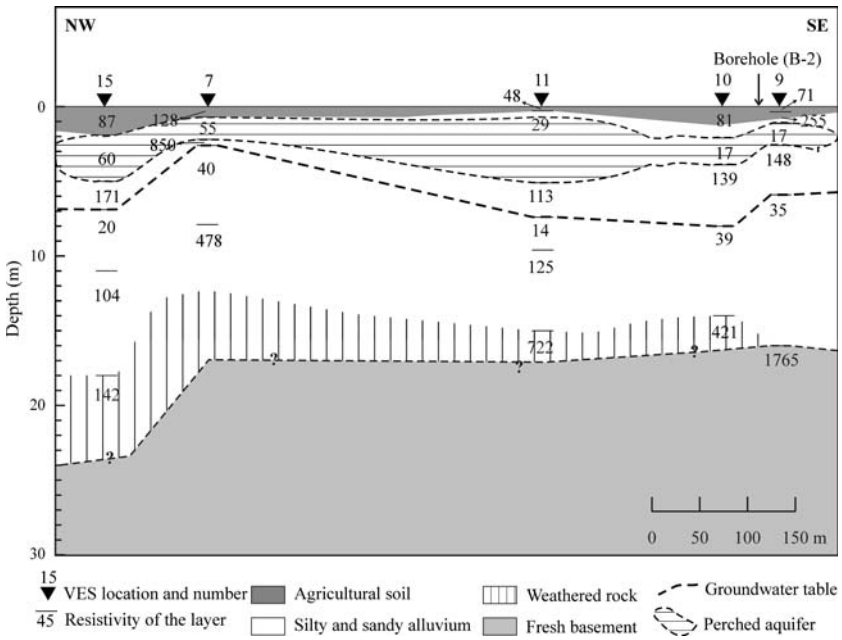

Fig. 7 A litho- and hydro-resistivity cross-section with a NW–SE trend, parallel to the river. The location is shown in Fig. 1b. Vertical exaggeration is ×16

between the two types of alluvium (a sandy layer and a silty layer) extends down to depths above the main groundwater table. This result shows that VES profiles can be a useful method to investigate the lateral and vertical variations of subsurface lithology as well as subsurface hydrology.

Low resistivity (55–90 Ωm) zones are observed at shallow depths (1–5 m) in both southwestern and northeastern areas (Fig. 5). These zones indicate the presence of a local perched aquifer or water-rich layer near the surface and above the main groundwater table. However, such a zone is not present in the southern part (Fig. 6), indicating lateral discontinuity of a perched aquifer. Figure 6 also shows that the northern part has a very low resistivity (17–29 Ωm) zone at shallow depth (1–5 m). Similarly, the near-surface perched aquifer extends laterally with a NW–SE direction in the central part of the study area (Fig. 7). These data also show the local and sporadic existence of unsaturated zones with relatively low to medium resistivities (113–850 Ωm) between the perched and main aquifers (Figs. 5, 6, 7); based on the borehole (B-2) data (Fig. 4), such zones indicate the presence of intercalated, massive sandy or silty layers. It is considered that the lateral continuation of a perched aquifer, which is likely parallel to

the present Geum River, may represent the vestige of an ancient river channel such as an oxbow lake. Within the ancient river channel, fine silty alluvium is preferentially deposited. Such a phenomenon was confirmed by Chae et al. (2004). They pointed out that the configuration of the river has changed and the main channel has moved westward by approximately 400 m over the past 80 years.

Interpreted-resistivity contour maps

Figure 8 shows six interpreted-resistivity contour maps at depths of 0 (surface), 5, 10, 15, 20, and 25 m, which were obtained by a kriging method with the Surfer software (Golden Software Inc). The VES-station locations are shown on the index map as small solid circles. At surface, the interpreted-resistivity systematically varies with a NE–SW direction (i.e. NW–SE trending zonal distribution) and increases toward the river (the southwestern part of the study area). It is noteworthy that such phenomenon roughly matches the spatial distribution of surface agricultural alluvium (i.e. low resistivity silty alluvium to the northeast and high resistivity sandy alluvium to the southwest). This indicates that the variation of surface resistivity is mainly controlled by the surface alluvium type.

On the 5 m-depth contour map, low resistivity (<20 Ωm) zones appear in the northeastern and central parts of the study area. On the other hand, such low resistivity zones occur at a depth of 10 m in the northwestern and southern parts and appear on the 15 m- and 20 m-depth contour maps in the southwestern part alongside the river (Fig. 8). As described above, the low resistivity zone near 5 m depth may reflect the presence of a perched aquifer, while those at deeper depths are interpreted to indicate the main aquifer. Thus, the spatial distribution of a low resistivity zone shows that the depth of the main aquifer generally increases toward the river. Using those contour maps (Fig. 8) and piezometric data (Fig. 2a), general flow paths of groundwater direct toward the river in the study area (Fig. 9). It is also inferred that the southward direction of the main groundwater flow locally changes to the southwest and southeast in the southern part of the study area, possibly due to the riverside revetment.

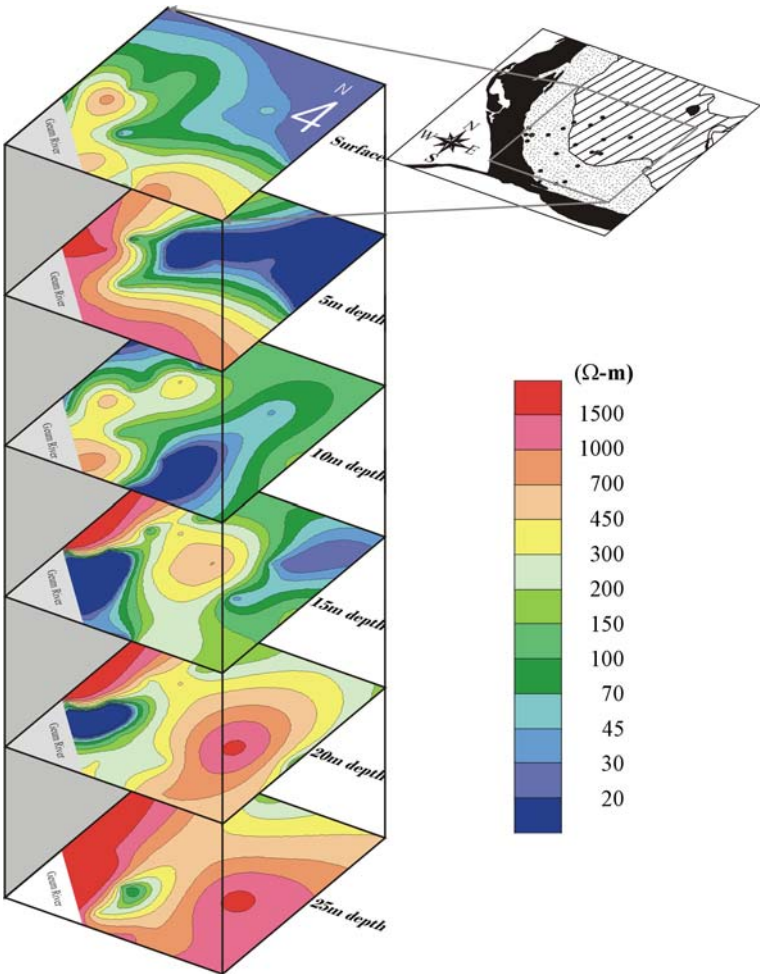

Fig. 8 Interpreted-resistivity contour maps at depths of 0 (surface), 5, 10, 15, 20, and 25 m. Kriging method was adopted for interpolation and extrapolation

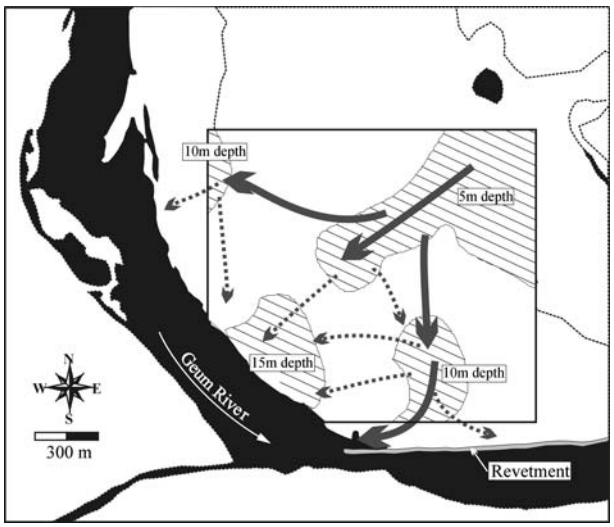

Fig. 9 Inferred groundwater flow directions in the study area. *Thick arrows* denote the direction of main groundwater flow; *dashed arrows* for minor flows. *Hatched areas* indicate very low resistivity (less 20 Ωm) zones at different depths (5, 10, and 15 m) on Fig. 8

A very high resistivity zone (more than 700 Ωm), indicating a fresh granitic basement, occurs below 15 m (in the western part) to 20 m (in the eastern part). Therefore, total thickness of alluvial sediments in the study area tends to generally decrease toward the riverside western part. This result may indicate the progressive westward migration of river channel (Chae et al. 2004). In the 25 m-depth contour map, an intermediate resistivity zone appears in the central part (Fig. 8), possibly indicating the presence of weathered basement rocks.

Comparison between VES and hydrochemical data

Water resistivities, ρ_w (in Ωm), were calculated from electric conductivities (in μS/cm) of groundwater samples, measured by Chae et al. (2004) in June 2002. Then, a contour map of ρ_w was drawn using a kriging (interpolation) method (Fig. 10b). Figure 10b clearly shows that the low water-resistivity (i.e. highly electrically conductive) zone is present adjacent to the river, corresponding to the occurrence of Group I waters in Fig. 10a. Group I waters occur in the area without a thick silt cover and are characterized by low pH and high concentrations of total dissolved solids (TDS), K, Ca, Mg, SO_4, and NO_3. Those waters represent the direct infiltration of surface pollutants associated with active agricultural activities (Chae et al. 2004). Therefore, the relatively lower ρ_w values in the southwestern part on Fig. 10b can be attributed to the higher concentrations of ionic contaminants in the groundwater. On the other hand, the area of Group III waters shows the relatively high ρ_w values due to the low TDS concentration, indicating the relatively low level of groundwater contamination. In the case of the area of Group II waters, the groundwaters were characterized by very low Eh values and very high Fe and Mn levels, indicating a strong anoxic environment (Chae et al. 2004). Nevertheless, the concentration of TDS in the Group II area falls between those in the other two areas because of very low NO_3 and SO_4 levels. The area of Group II waters corresponds to the area of intermediate water resistivity in Fig. 10b. These results reveal that the ρ_w contour map may represent the concentration of TDS as an effective indicator of the degree of groundwater contamination.

Based on the interpreted-resistivities of main aquifers derived from VES data, another contour map (Fig. 10c) was drawn using the kriging method and was compared with the ρ_w contour map. Ebraheem et al. (1997) reported the close correlations among the earth resistivity estimated from VES soundings, the water resistivity converted from EC (electrical conductivity) of groundwater, and the concentration of TDS. Based on such observations, they suggested that the VES data can be useful to trace the contaminated groundwater zone and fresh-/brackish-/saline-water interfaces in the Nile Delta. In the present study, however, the earth resistivity contour map of the main aquifer reveals the spatial pattern different from the ρ_w contour map (Fig. 10c). Therefore, it is suggested that the earth resistivity of an aquifer cannot directly reflect the water chemistry (and contamination) in the study area.

For the study area, three possible explanations can be considered for the difference between the aquifer's earth resistivity and the water resistivity. Firstly, a time factor as a yearly basis can be considered, because the VES survey for this study was conducted in September–October 2003, while the hydrochemistry data in Chae et al. (2004) as the source of water resistivity calculation was collected in June 2002. However, a significant change of groundwater chemistry in 1 year seems unlikely because the spatial distribution of groundwater chemistry was not significantly changed within a time span from September 2001 to June 2002 (see Fig. 4 of Chae et al. 2004). Secondly, a seasonal factor can be considered because the VES survey was carried out in the post-monsoon season (September–October) after heavy rainfall events, while the hydrochemistry data was during the pre-monsoon season (June) without heavy rainfall. As discussed above, the water chemistry in the sandy alluvium area adjacent to the river (i.e. southwestern part of the study area) is sensitive to the precipitation and therefore a larger amount of rainwater with a relatively low concentration of TDS can penetrate more preferentially through such sandy alluvium area into the main aquifer. However, this explanation cannot be successfully applicable to the central part, where a thick silty alluvium occurs but shows the high earth resistivities. Thirdly, a fundamental consideration can be raised. The

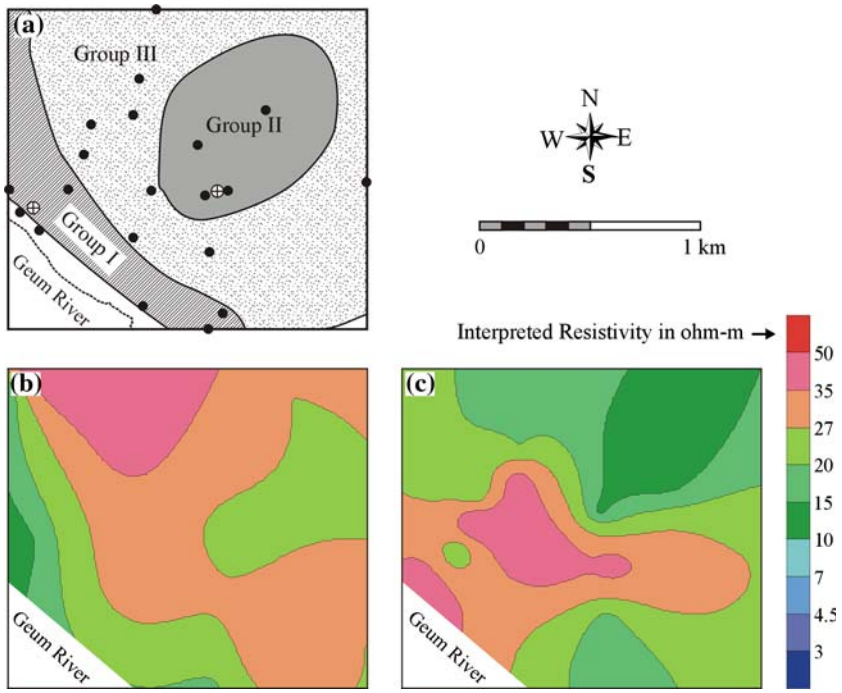

Fig. 10 **a** A map showing spatial distribution of the clustered hydrochemical groups (after Chae et al. 2004). Contour maps of **b** water resistivity (ρ_w) and **c** earth resistivity of the main aquifer are shown for comparison

values of TDS, EC, and ρ_w were directly obtained from groundwater samples, whereas the earth resistivity was obtained from measurements on the land surface. It is generally known that even the earth resistivity of the aquifer is affected by not only water chemistry but also soil type and porosity (McNeill 1980). Especially, when the water chemistry varies widely, such as the case of the seawater intrusion into a fresh aquifer with a homogeneous lithology, the earth resistivities may show a significant enough contrast to delineate the extent of groundwater contamination (e.g. Steinich and Marin 1996; Ebraheem et al. 1997; Choudhury and Saha 2004). Considering the heterogeneity of surface and subsurface geology and the relatively narrow variation of ρ_w (13–48 Ωm) in the study area, the spatial distribution of resistivities shown in Fig. 10c is likely to reflect more significantly in the spatial variation of grain size or aquifer lithology rather than the water chemistry.

Hydrogeologic environment and groundwater contamination

The identified hydrogeologic environment of the study area, based on the VES data and borehole lithologies, can be summarized as follows. Two types of aquifers are present in the riverside alluviums of the study area: the perched aquifer and the main aquifer. The perched aquifers occur at shallow depths (1–5 m deep) in the central and southwestern parts of the study area (Figs. 5, 6). The perched aquifer in the central part extends along a NW–SE direction, parallel to the river (Fig. 7) and is to be developed along an ancient channel. This vestige of an ancient channel is characterized by the occurrence of a thick clay-rich silty soil. The silty soil is considered to have been deposited in a floodplain environment and may hinder the oxygen (and rainwater) from deep infiltration into alluvium. Therefore, the main aquifer in the central part is below such a perched aquifer and thus has a strong anoxic condition to result in the low Eh values and high Fe and Mn levels in groundwaters. The very low NO_3 level of Group II waters in the central part is due to denitrification related to such anoxic condition (Chae et al. 2004). On the other hand, in the southwestern part adjacent to the river, the perched aquifer does not occur. The main groundwater table in the area occurs at the moderate depth range (3–12 m deep) but generally becomes shallower toward the river. During the flow of the main groundwater toward the river in the southwestern part, mixing of a large amount of contaminants (e.g. NO_3, SO_4, etc.) occurs due to their infiltration through the surface sandy alluvium with high permeability. This process can be confirmed by the integration of water resistivity, hydrochemistry, and the general flow paths of the groundwaters (Figs. 9, 10).

Borehole lithology data show that the main aquifer materials in the study area are composed of silt and fine- to coarse-grained sand in the upper (shallower) alluvium, and of pebble in the deeper alluvium (Figs. 3, 4). Such spatial change of the aquifer materials seems to strongly affect the earth resistivity change, while water resistivity is mainly controlled by the chemistry and TDS concentration of

groundwaters. It has been reported that fine-grained sand has the minimum resistivity among various kinds of aquifer materials, such as clay, silt, and sand in the alluvial environment (Choudhury and Saha 2004). Therefore, it is assumed that the aquifer materials in the southern and northern parts on Fig. 10c, where the main aquifer's earth resistivities are the lowest values, are mainly composed of fine-grained sand. The present study shows that the geoelectric sounding survey complemented with borehole lithology and hydrochemistry data can be used as an inexpensive and efficient method for delineating the subsurface hydrogeology in alluvial environment.

Summary and conclusions

Riverside alluviums have recently become the preferential site of large-scale groundwater development such as bank filtration. However, alluvial groundwater in Korea is severely contaminated by pervasive agricultural activities. The integration of VES data with borehole lithology provides information on the subsurface condition of riverside alluvium. Especially, the resistivity profiles and cross sections, calibrated with borehole data, show the vertical and lateral change of subsurface hydrolithology, which are very crucial to understand the chemistry and quality of alluvial groundwater (Min et al. 2003; Chae et al. 2004). To examine the applicability of the VES survey to the contamination study in the riverside alluvium setting, 20 VES profiles were obtained in a riverside alluvium at the Buyeo area, Korea, on which excessive agrochemicals are used, and were interpreted by combining with borehole logs and hydrochemical data. Some important results were deduced from this study as follows.

The depth of the main groundwater table in an alluvial aquifer becomes slightly deeper toward the river, indicating the overall groundwater flow toward the river. The surface resistivity contour map reveals that the electrical resistivity largely varies in a NE–SW direction with a general increase toward the river. This pattern agrees well with the spatial distribution of surface alluvium (i.e. silty alluvium in the NE part, while dominantly a sandy alluvium in the SW part near the river), indicating that the spatial variation of surface resistivity is mainly controlled by the surface soil (alluvium) type. The boundary between a sandy alluvium and a silty alluvium extends down to the level of the main groundwater table. Chae et al. (2004) showed a lithologic control of the chemistry (and agrochemical contamination) of alluvial groundwater in the study area, i.e., severely contaminated (TDS-rich) groundwater preferentially occurs in the area of surface sandy alluvium. Although, water resistivity correlated with the TDS in groundwater, its distribution pattern did not match with that of the earth resistivity of the aquifer. In other words, the earth resistivity of aquifer varied in accordance with the variation of soil type rather than the groundwater chemistry change. Therefore, the earth resistivities should be carefully interpreted along with the consideration of hydrochemistry data, especially in the places where groundwater chemistry changes considerably within a narrow space range, such as in riverside alluviums with complex subsurface geology.

Acknowledgments This study was supported by the Korea Research Foundation (KRF) through the Environmental Geosphere Research Lab (EGRL) of Korea University. Dr. Mark Bultman is gratefully acknowledged for his helpful suggestion and editing the manuscript. The authors thank many students in Korea University for their assistance in the field survey.

References

Burt TP, Matchett LS, Goulding WT, Webster CP, Haycock NE (1999) Denitrification in riparian buffer zone: the role of floodplain hydrology. Hydrol Process 13:1451–1463

Chae GT, Kim K, Yun ST, Kim KH, Kim SO, Choi BY, Kim HS, Rhee CW (2004) Hydrogeochemistry of alluvial groundwaters in an agricultural area: an implication for groundwater contamination susceptibility. Chemosphere 55:369–378

Choudhury K, Saha DK (2004) Integrated geophysical and chemical study of saline water intrusion. Ground Water 42:671–677

Ebraheem AM, Senosy MM, Dahab KA (1997) Geoelectrical and hydrogeochemical studies for delineating ground-water contamination due to salt-water intrusion in the northern part of the Nile Dela, Egypt. Ground Water 35:216–222

Edet AE, Okereke CS (2002) Delineation of shallow groundwater aquifers in the coastal plain sands of Calabar area (Southern Nigeria) using surface resistivity and hydrogeological data. J Afr Earth Sci 35:433–443

El Gamili MM, Ibrahim EH, Hassaneen ARG, Abdalla MA, Ismael AM (2001) Defunct Nile Branches inferred from a geoelectric resistivity survey on Samannud area, Nile Delta, Egypt. J Archaeol Sci 28:1339–1348

Fred GB (1993) Engineering geology. University of Natal, Durban

Kim HS, Seo MC, Lee CW, Jin SH (2003) A high-resolution geophysical survey on the alluvium aquifer in the Gunsuri, Buyeo (Guem river) using the seismic and GPR methods. Paper presented at the 2003 Spring meeting of Korea society of soil and groundwater environment [in Korean with English abstract], Seongnam, Korea, 18–19 April 2003, pp 287–291

Kraft GJ, Stites W, Mechenich DJ (1999) Impacts of irrigated vegetable agriculture on a humid north-central US sand plain aquifer. Ground Water 37:572–580

McNeill JD (1980) Electrical conductivity of soils and rocks, Technical Note TN-5, Geonics Limited, Missisauga

Min JH, Yun ST, Kim K, Kim HS, Kim DJ (2003) Geologic controls on the chemical behavior of nitrate in riverside alluvial aquifers, Korea. Hydrol Process 17:1197–1211

Parasnis DS (1997) Principles of applied geophysics. Chapman & Hall, London

Pozdnyakova L, Pozdnyakov A, Zhang R (2001) Application of geophysical methods to evaluate hydrology and soil properties in urban areas. Urban Water 3:205–216

Rhee CW, Kim HS, Lee KJ (2002) Delineation of internal heterogeneities of Keum River point bar deposits in Buyeo area using

GPR data [in Korean with English abstract]. J Korean Geophys Soc 5:337–344

Steinich B, Marin LE (1996) Hydrogeological investigations in Northwestern Yucatan, Mexico, using resistivity surveys. Ground Water 34:640–646

Yang CH, Lee WF (2002) Using direct current resistivity sounding and geostatistics to aid in hydrogeological studies in the Choshyichi alluvial fan, Taiwan. Ground Water 40:165–173